CrystEngComm

Accepted Manuscript

ROYAL SOCIETY OF CHEMISTRY

www.rsc.org/crystengcomm

Journal Name

ARTICLE

Werner clathrate formation with polyaromatic hydrocarbons: comparison of different crystallisation methods

4Received 00th January 20xx,
Accepted 00th January 20xx

DOI: 10.1039/x0xx00000x

www.rsc.org/

Merrill M. Wicht,[a,b] Hong Su,[a] Nikoletta B. Báthori*[b] and Luigi R. Nassimbeni[a]

The single crystal structures of the Werner host, bis-isothiocyanato tetrakis-vinylpyridine nickel (II), **H**, with seven polyaromatic hydrocarbons (PAHs), indene (**IND**), naphthalane (**NAP**), azulene (**AZU**), fluorene (**FLU**), anthracene (**ANT**), phenanthrene (**PHE**) and pyrene (**PYR**) have been elucidated. These structures were scrutinised for isomorphous and isostructural behaviour. The inclusion compounds can be formed using a variety of crystallisation methods such as solution crystallisation, grinding, slurrying and co-melting methods. Grinding allowed determination of rate constants of formation for the host with **NAP** at room temperature and with **AZU** at 35°C. The kinetics of thermal decomposition of the inclusion compounds using non-isothermal methods permitted the establishment of the activation energies of the decomposition reactions with **NAP** and **IND**. Product formation in an ambient water slurry was successful with guests **NAP** and **AZU** showing low solubility at room temperature; for **PHE**, **PYR** and **FLU** this occurred only after longer stirring at a higher temperature (50°C) at which the guests had low levels of solubility and for **ANT** no successful slurrying results were reached.

Introduction

'Green' or 'sustainable' chemistry, based on product design without the generation of hazardous substances, is an effective manner of inclusion complex preparation.[1] Generally, crystallisation of an inclusion compound is conducted by dissolution of the host and guest compounds in a suitable inert solvent, followed by the formation of crystals using slow solvent evaporation. Simplification of experimental procedures and minimisation of labour costs for industrial applications, make solid-solid reactions attractive. Inclusion complexation can occur by mixing and grinding powdered compounds in a solid-state reaction.[2] The progress of these solid-state reactions can be monitored using suitable measurements such as infra-red or ultra-violet spectroscopy or powder X-ray diffraction (PXRD).

Mechanochemical synthesis (manual grinding or ball milling) has been applied to the construction of metal-ligand coordination bonds as well as non-covalent interactions in supramolecular chemistry such as hydrogen bonds, halogen bonds and π···π interactions.[3] Various methods of cocrystallisation such as neat grinding, crystallisation from the melt, solution growth and slurrying have been compared with single crystal analysis. Neat grinding is independent of solubility effects resulting in the avoidance of solubility and solvent competition encountered in solution crystallisation.[4] Two other processes are slurrying with a suitable solvent and melt crystallisation. The melt process allows the guest compound to be heated and then melted into the host compound. If the host does not decompose on heating, crystallization can be performed by melt cooling. In slurrying, the process is favoured when solution evaporation results in solvent inclusion or co-crystal formation.[5]

Successful solvent-free reactions have been promoted despite the limitations of solid-solid reactions. Often products of solid-state reactions differ from those obtained in the solution phase due to spatial orientation or packing of the crystalline material. However, an ordered structure can be obtained by simply mixing components thoroughly to form host-guest systems.[2] Solid-vapour inclusion formations with Werner clathrates have received little attention although they have been considered by Lusi and Barbour in the separation of isomers[6] where the sorption properties of three Werner clathrates were investigated and the mechanochemical processing produced homogeneous solid solutions.[7]

Polycyclic aromatic hydrocarbons (PAHs), consisting of two or more unsubstituted aromatic fused rings are the result of

[a] University of Cape Town, Rondebosch, Cape Town, South Africa. Tel: 27 21 6505893; Fax: 27 21 650541
[b] Cape Peninsula University of Technology, Zonnebloem, Cape Town, South Africa. Tel: 27 21 4608354; E-mail: bathorin@cput.ac.za
† Footnotes relating to the title and/or authors should appear here.
Electronic Supplementary Information (ESI) available: [details of any supplementary information available should be included here]. See DOI: 10.1039/x0xx00000x

incomplete burning of coal, oil and gas and other organic substances. They are a class of environmental pollutants with carcinogenic properties.[8] Apart from the zeolitic channel sorption of anthracene,[9] the structures of aromatic hydrocarbons as guests in inclusion compounds have not been considerably scrutinised. The development of simple and low cost methods for quantitative recovery of PAHs from solution is a challenging task[10] due to their variety of sizes, shapes and properties.[11] The host 3,5-dinitrobenzonitrile forms clathrates with various hydrocarbons and aza donor molecules, with their host network yielding 3D channels filled by guest molecules.[12] The structures of a series of PAHs as guests in clathrates formed by head-to-tail hydrogen bonding links in a xanthenol host have been elucidated[13] and the solid-solid reaction kinetics were monitored by PXRD. More recently, host compounds derived from dipyridyl linkers and arylboronate esters have been shown to capture a variety of PAHs, and were employed to sequester specific hydrocarbons from a mixture. PAH inclusion selectivity is related to size-fitting adaptations to the octahedral-shaped cavity formed through CH•••π interactions of the host.[14] The structures of PAHs as guests in Werner hosts are represented in the Cambridge Structural Database[15] in only seven cases. These include naphthalene as well as bromonaphthalene and azulene in layered clathrate structures with $Ni(NCS)_2(4\text{-methylpyridine})_4$ by Lipkowski and co-workers.[16] Having previously considered selectivity of xylene isomers with an isoquinoline-based Werner host,[17] we now present the results of inclusion compounds formed between the Werner host bis-(isothiocyanato) tetrakis-vinylpyridine nickel(II), **H**, with the PAHs shown in Scheme 1.

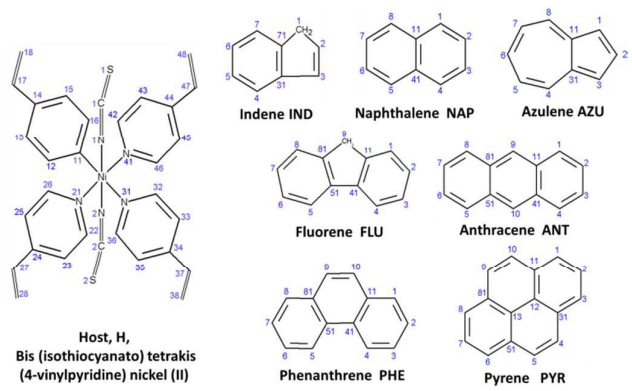

Scheme 1 Structural line diagrams and atomic numbering of the host, $Ni(NCS)_2(4\text{-vinylpyridine})_4$ and the seven polycyclic aromatic hydrocarbon guests

This compound is an example of a Werner host, of general formula MX_2L_4, where M is a divalent metal cation (e.g. Ni(II), Co(II), Fe(II), Cu(II) and Mn(II)), X is an anionic ligand (NCS^-, NCO^-, CN^-, NO_3^- or halide), and L is a substituted pyridine or α-arylalkylamine. These compounds have the ability to enclathrate a variety of guests and can display distinct selectivity.[18,19,20] The structures of the host **H** as the apohost, as well as those of its inclusion compounds with the isomers of xylene, have been interpreted.[21,22] In addition, thermal and structural studies of this host with halogenated methanes[23,24] and cyclic hydrocarbons[25] have been carried out. Recently the structures of three Werner complexes have been analysed in terms of their packing, and the results confirmed that nickel(II) thiocyanato complexes relate their crystal design to relatively weak forces such as hydrogen bonding or π•••π interactions especially with pyridine derivatives or other similar ligands.[26]

Compared with our previous work,[17] in which the rigidity of the isoquinoline ligand was found to play an important role in selectivity, the properties of this more flexible ligand, 4-vinylpyridine, are investigated. Here the crystal structures of the host, **H**, $Ni(NCS)_2(4\text{-vinylpyridine})_4$ with each of the seven polyaromatic hydrocarbon guests: indene (**IND**), naphthalene (**NAP**), azulene (**AZU**), fluorene (**FLU**), anthracene (**ANT**), phenanthrene (**PHE**) and pyrene (**PYR**) were obtained from solvent crystallisation. These Werner clathrates were also synthesised via other methods (neat grinding, slurrying and melting) and their formation and decomposition kinetics are discussed.

Results and discussion

Crystal Structures

Between the nine crystal structures, summarised in Table 1, a number of similarities were found. The structures of **H•IND**, **H•NAP** and **H•AZU** are isomorphous and crystallise in the space group $Pna2_1$ with Z=4. The asymmetric unit of **H•IND**, comprising one host and two guests is shown in Fig. 1(a) and the packing shown along [001] in Fig 1(b) has the guest molecules lying in crossed channels which run along [010] and [001]. The void spacing in Fig 1(c) shows these crossed channels depicted by the blue arrows. The structure of **H•NAP** is analogous with that of **H•IND.** However, although **H•AZU** is isomorphous, the azulene guests are disordered and are located about pseudo centres of symmetry, with partial site occupancies of 0.808(7) / 0.192(7) and 0.783(8) / 0.217(8).

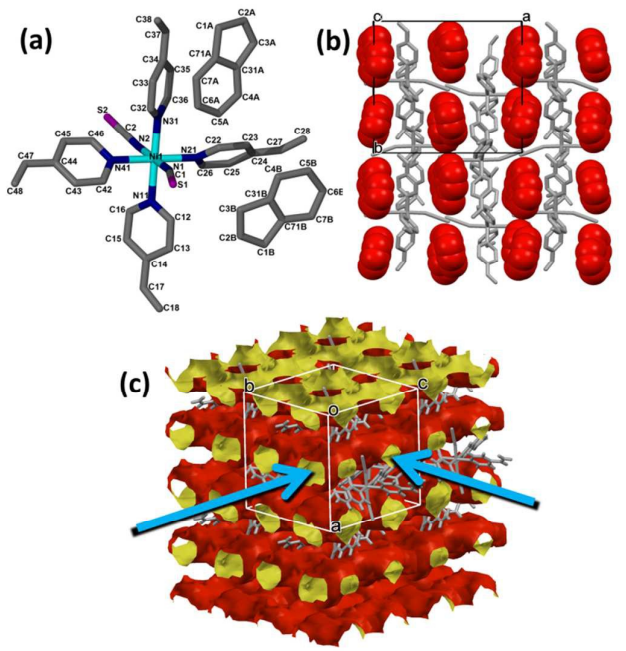

Figure 1 (a) Asymmetric unit of **H•IND** (Hs omitted for clarity); (b) packing down [001] showing the indene molecules occupying the channels in red spacefill model; (c) Void spacing of **H•IND** viewed down the apex to show the crossing channels down [100] and [010] with blue arrows

The structures obtained with fluorene as guest, gave rise to crystals of distinctly different habits, namely plates (**H•FLU(I)**) and blocks, (**H•FLU(II)**). Phenanthrene also forms two different crystal structures, labelled **H•PHE** and **H•PHE•BEN**; the latter containing benzene as second guest. **H•FLU(I)** and **H•PHE** form an isomorphous pair each with two hosts and 1.5 guests in the asymmetric unit. The packing diagram of **H•FLU(I)** is shown in Fig. 2(a), viewed down [100]. One guest molecule, labelled **A**, is ordered and located in a general position. The second guest molecule, **B**, is disordered by translation along the *b* axis, and occupies positions which straddle both centres of inversion at Wyckoff position *a* and *d*. **H•FLU(I)** forms 3-way channels down the central diagonal axis.

H•PHE•BEN crystallises with two host, one phenanthrene and one benzene molecules in the asymmetric unit with all moieties ordered. The phenanthrene and benzene molecules are in channels along both [100] and [010] shown in Fig 2(b) with the phenanthrenes depicted in green and the benzenes in blue spacefill models. **H•ANT** crystallises with two hosts and half an anthracene in the asymmetric unit. The anthracene is translationally disordered along the *a* axis, covering Wyckoff positions *c* and *e*, shown in Fig 2(c) viewed down [100]. The position of the phenanthrene guest in **H•PHE•BEN** enforces a 2Å longer *c* axis than in **H•ANT**, hence they are not isostructural.

The asymmetric unit of **H•FLU(II)** comprises four hosts in general positions and two guests, both translationally disordered along the *a* axis. The host molecules display disorder of the NCS and some vinyl moieties. The guests are crystallographically independent, positioned on Wyckoff positions *a* and *d* (illustrated in dark blue in Fig. 2(d)); and the other on Wyckoff positions *g* and *h* (illustrated in light blue in Fig. 2(d)). The translational disorder of the guests is shown down [010] in Fig. 2(e).

H•PYR.MeOH crystallises with one host, two pyrene and 0.5 methanol in the asymmetric unit. The host and pyrene molecules are ordered except for one vinyl group showing disorder. The methanol is disordered and lies near a centre of inversion at Wyckoff position *c*. The packing is shown in Fig. 2(f), viewed down [010]. The pyrenes are illustrated in purple and the methanols in yellow spacefill.

Journal Name

ARTICLE

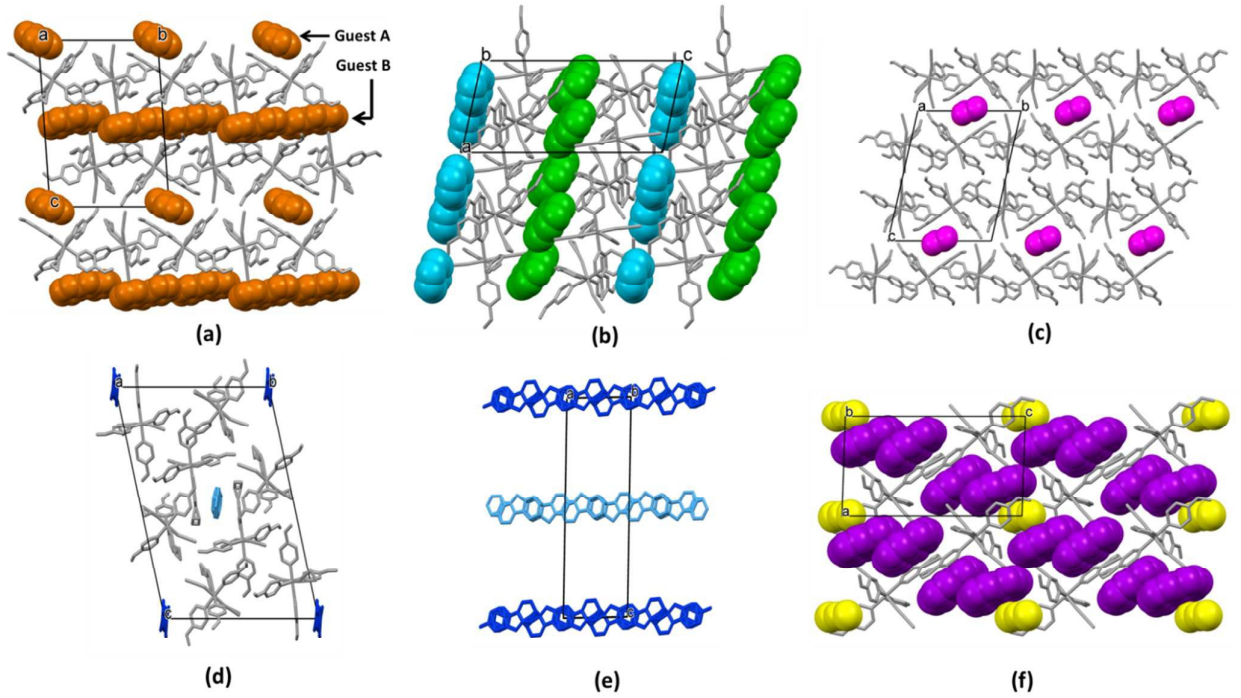

Figure 2 **(a)** Packing diagram of **H•FLU(I)** down [100] with the guests in orange spacefill model. (**Guest A** – ordered, **Guest B** – disordered); **(b)** Packing of **H•PHE•BEN** (**PHE** in green, **BEN** in blue spacefill); **(c) H•ANT** down [100] (disordered **ANT** in magenta spacefill); **(d)** Packing diagram of **H•FLU(II)** with disordered **FLU** viewed edge-on down [100]; (**e**) The disorder of **FLU** in **H•FLU(II)** shown down [010] (the two independent guests are in different shades of blue and **(f) H•PYR•MeOH** down [010] (**PYR** in purple and **MeOH** in yellow spacefill models)

Journal Name

ARTICLE

Table 1 Crystallographic data

	H•IND	H•NAP	H•AZU	H•FLU(I)	H•PHE	H•FLU(II)	H•ANT	H•PHE•BEN	H•PYR•MeOH
Chemical Formula	$Ni(NCS)_2(C_7H_7N)_4$• $2(C_9H_8)$	$Ni(NCS)_2(C_7H_7N)_4$• $2(C_{10}H_8)$	$Ni(NCS)_2(C_7H_7N)_4$• $2(C_{10}H_8)$	$4Ni(NCS)_2(C_7H_7N)_4$• $3(C_{13}H_{10})$	$Ni(NCS)_2(C_7H_7N)_4$• $⅝(C_{14}H_{10})$	$4Ni(NCS)_2(C_7H_7N)_4$• $(C_{13}H_{10})$	$2Ni(NCS)_2(C_7H_7N)_4$• $⅞(C_8)$	$2Ni(NCS)_2(C_7H_7N)_4$• $(C_{14}H_{10})$•(C_6H_6)	$2Ni(NCS)_2(C_7H_7N)_4$• $4(C_{16}H_{10})$• (CH_3OH)
Formula weight	827.72	851.74	851.84	2880.61	706.80	2537.71	1275.03	1447.12	2032.05
Temperature/K	173(2)	173(2)	173(2)	173(2)	173(2)	173(2)	173(2)	173(2)	173(2)
Crystal System	Orthorhombic	Orthorhombic	Orthorhombic	Triclinic	Triclinic	Triclinic	Triclinic	Triclinic	Triclinic
Space group (no.)	$Pna2_1$ (no. 33)	$Pna2_1$ (no. 33)	$Pna2_1$ (no. 33)	$P\bar{1}$ (no. 2)	$P\bar{1}$ (no. 2)	$P\bar{1}$ (no. 2)	$P\bar{1}$ (no. 2)	$P\bar{1}$ (no. 2)	$P\bar{1}$ (no. 2)
a/Å	16.9052(11)	16.8137(18)	16.7378(12)	10.3322(10)	10.3117(8)	10.1821	10.1289(4)	10.4819(9)	10.9587(7)
b/Å	15.7416(10)	16.1198(19)	16.1297(12)	16.8462(10)	16.8992(14)	23.1916	16.4770(9)	16.8458(14)	12.1349(8)
c/Å	16.3948(11)	16.3865(19)	16.4588(12)	22.134(2)	22.3884(17)	28.6186	20.6537(10)	22.5690(5)	19.7621(12)
α/º	90.00	90.00	90.00	84.603(2)	81.874(2)	74.602	100.430(2)	100.059(2)	93.9070(10)
ß/º	90.00	90.00	90.00	84.385(3)	83.128(2)	85.683	97.129(3)	100.131(2)	91.4260(10)
γ/º	90.00	90.00	90.00	74.788(3)	76.007(10)	81.596	105.351(3)	102.908(2)	97.8780(10)
V/Å^3	4362.9(5)	4441.3(9)	4443.5(6)	3690.3(5)	3732.8(5)	6440.7	3214.8(3)	3727.6(5)	2595.6(3)
Z′/Z	1 / 4	1 / 4	1 / 4	½ / 1	2 / 4	1 / 2	1 / 2	1 / 2	½ / 1
$D_{calc.}$/Mg m^{-3}	1.260	1.274	1.273	1.296	1.258	1.314	1.322	1.289	1.300
Radiation type	MoKα	MoKα	MoKα	MoKα	MoKα	MoKα	MoKα	MoKα	MoKα
F(000)	1736	1784	1784	1504	1475	2656	1334	1512	1062
Crystal size/mm	0.44x0.38x0.37	0.25x0.20x0.07	0.38x0.31x0.20	0.23x0.15x0.04	0.22x0.18x0.03	0.26x0.19x0.18	0.20x0.18x0.09	0.48x0.34x0.32	0.50x0.40x0.20
Colour, Crystal form	Violet, Chunk	Violet, Chunk	Dark Blue, Chunk	Violet, Plate	Violet, chunk	Violet, Block	Violet, Block	Violet, Chunk	Violet, Chunk
Total reflections	87546	32257	74997	94121	39815	156695	24868	89108	98932
Unique reflections	10914	10039	10650	14995	16209	32284	13088	17210	13093
$\Theta_{min-max}$/º	1.77 /28.42	1.75 / 28.37	1.75/ 27.95	2.87 / 26.39	2.04/27.09	1.48 / 28.43	2.12 / 26.37	2.23 / 26.41	1.92 / 28.54
$R[F^2>2\sigma(F^2)];wR(F^2);S$	0.0354;0.0939;1.040	0.0424;0.074;1.003	0.0276;0.0611;1.014	0.0496;0.0911;1.001	0.0561;0.1454;1.015	0.1101;0.2973;1.033	0.0635;0.1919;1.003	0.0445;0.1254; 1.022	0.0365;0.1056;1.027
Parameters/ data	515/10914	533/10039	607/10650	986/14995	968/16209	1583/32284	764/13088	894/17210	679/13093
Res. Peak (max/min)/eÅ^{-3}	0.700/-0.651	0.213/-0.254	0.219/-0.246	0.538/-0.259	0.688/-0.447	1.283/-1.736	0.816/-0.515	0.868/-0.387	0.787/-0.339

Journal Name

ARTICLE

Mechanochemical synthesis

Environmentally attractive solid-solid reactions are a well-known format for generating multicomponent crystals or cocrystals. Rastogi[27,28] discussed the kinetics of solid-solid reactions between selected hydrocarbons and picric acid. Principal mechanisms for the formation of cocrystals have been established as surface migration and diffusion through the vapour phase of the aromatic hydrocarbon.[4] Braga *et al.*[29] relates the interactions between the components to be diffusion controlled, or in the case of co-grinding, an intermediate eutectic phase is formed. In our case this would involve π stacking of the aromatic rings of the guest and the Werner host.

Solid-solid reactions were carried out between the **H** and all solid guests by grinding stoichiometric quantities of the solids in a mortar at 298 K or at a higher temperature in a brass mortar. The reactions were monitored by interrupting grinding at given periods and adding a fixed quantity of diamond powder to the sample before PXRD analysis. Certain reflections associated with the starting materials decrease in intensity while those of the new compound increase in intensity based on the time of grinding. Successful agreement between the single crystal structure and ground products were reached with the guest **NAP** at room temperature and **AZU** at 35°C. All other guests did not show correspondence between the two methods.

In Figure 3 we present the **NAP** diffraction patterns as shown: the computed pattern derived from the single crystal structure of **H•NAP** (A), the host, **H** (B), **NAP,** the guest (C), the sample after 15 minutes of grinding (D), and the pattern after a slurry experiment was performed (E). (*PXRD patterns for these grinding experiments are in the ESI, Figures S1 to S2).*

The vapour pressure of the guest is critical in the effectiveness of a grinding experiment. Of the guests, with the exclusion of **IND** (l), **NAP** has the lowest melting point of 80 - 82°C and its higher vapour pressure influences the amount of diffusion occurring on grinding. The shaded sections in the PXRD pattern in Fig 3 indicate a number of peaks of interest. When **Peak 1** (9.3° at 2θ) and **Peak 2** (21.1°) were monitored, a gradual increase during grinding was observed. However, the decrease in intensity of **Peak 3** at 12.6° during the grinding process (relative to (111) peak of diamond at 44.1° 2θ) is shown in Figure 4, as a plot of *ln(peak intensity)* vs *time*. This yielded a straight line (**A**) indicating a first order reaction with a rate constant of 0.137 min^{-1} and a half-life of 5.06 mins.

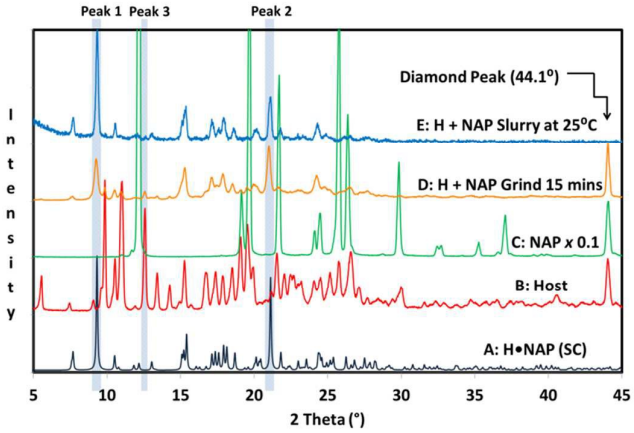

Figure 3 PXRD profiles: A: **H•NAP** generated pattern; B: pure **host**; C: pure **NAP**; D: **H + NAP** after 15 minutes grinding at RT; and E: slurry experiment at 25°C. The grey highlights show the peaks of interest and the peak at 44.1° 2 theta is the diamond internal standard peak

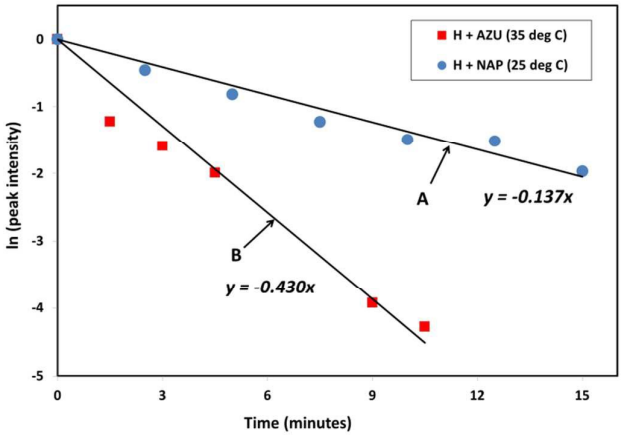

Figure 4 Kinetics of the grinding reactions between host **H** and **NAP** at 25°C (**A**), and **H** and **AZU** at 35°C (**B**).

The vapour pressures of the solid guests were considered at temperatures of 25 and 50°C in an attempt to predict the outcome of the grinding experiments.[30,31] Grinding **H** with **NAP**, (vapour pressure of 11.5 Pa at 25°C) was successful at room temperature. At 50°C (75.8 Pa), co-grinding of **H** and **NAP** produced the final product after just 2.5 minutes. As **AZU** was deemed to require a slightly higher temperature to reach an acceptable vapour pressure (11.1 Pa at 35°C), favourable grinding in a brass mortar at 35°C was achieved. The **AZU** peak at 11.6° decreased in intensity as shown in Figure 4, plot **B**, giving a rate constant of 0.430 min^{-1} with a half-life of 1.61

minutes. This is a good example to highlight the importance of vapour pressure and the significance of gas phase diffusion in these grinding experiments.

Slurry Experiments

Stoichiometric amounts of the host and guest were placed in a vial and 1 mL of distilled water added to the mixture. This was stirred (550 rpm, 54 hours at 25ºC) and the slurry was filtered and dried prior to analysis by PXRD. The **H•NAP** pattern obtained from the slurry experiment is labelled **E** (Fig 3). **Peak1** and **Peak2** appeared while **Peak3** (12.5º 2θ) has completely disappeared. Pattern **E** agrees well with that of the **H•NAP** crystal. The solubility of both the **H** and the guest (0.003 %m/m at 25ºC)[30,31] in water (S_w) is low thus water is a suitable solvent for the slurry experiment. Similarly, the product formation with **H** and **IND** was also successful. In the case of **H** and **AZU,** (S_w=0.002 %m/m at 25ºC), a number of corresponding peaks between the slurry product and the generated pattern were found.

Slurry experiments with the other guests were carried out for 72 hours at 50ºC. In the case of using **PHE** (S_w=4.0x10^{-4} %m/m, 50ºC) as a guest, partial agreement with the crystal was noted (peak at 8º 2θ). In the same way, a peak for **PYR** (S_w=9.0x10^{-5} %m/m, 50ºC) at 21.8º 2θ and for **FLU** (S_w=6.0x10^{-4} %m/m, 50ºC) at 8º 2θ, indicated that the experiment was partially successful. Guest **ANT** (S_w=4.5 x 10^{-6} %m/m, 25ºC) was not successful in this experiment even with stirring at a higher temperature (50ºC) for 96 hours. (*PXRD patterns of the slurry experiments are in the ESI, Figures S3 to S8).*

Co-melting

Co-melting was performed on a hot-stage microscope. The melt mixture was left at 92ºC for 10 mins. The PXRD analysis revealed that the product is a physical mixture of the starting materials.

Kinetics of thermal decomposition

The kinetics of thermal decomposition were measured for **H•NAP** and **H•IND** using the method of Flynn and Wall[32] , in which the mass losses of the compound were recorded at various heating rates varying from 2 to 32 Kmin^{-1}. These non-isothermal thermogravimetric curves for **H•NAP** are shown in Fig. 5 and for **H•IND** in *ESI, Fig. S10*.

The decomposition occurred in three stages: Stage 1 was due to the loss of the two guests, while stage 2 and 3 could each be attributed to the loss of pairs of vinyl pyridine ligands. In **H•NAP** the guest is found in channels along [010] and [100] and forms an intercalate structure with a high guest to host ratio; thus the thermal stability and kinetics of decomposition are expected to be lower than the loss of the ligands from the host compound (Table 2).

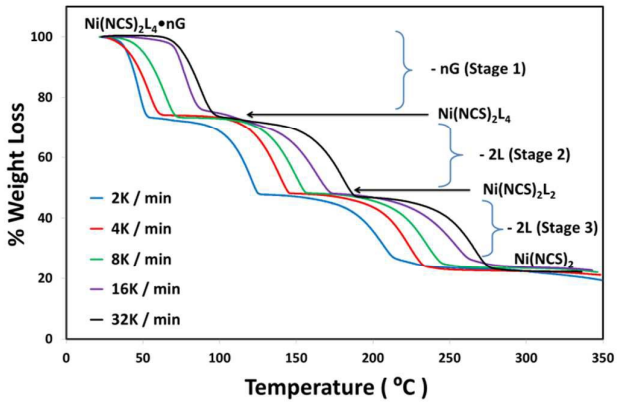

Fig 5 Non-isothermal TG curves for **H•NAP** (L = NAP)

For Stage 1 the corresponding mass losses and activation energies were calculated over α ranges for the inclusion compounds and are indicated in Table 2**.** The extent of reaction is defined as

$$\alpha = (m_t - m_0)/(m_\infty - m_0)$$

with m_0 = initial mass, m_t=mass at time *t* and m_∞=final mass. Plots of log β/β_o *vs.* 1/*T* for the **H•NAP** where β is the heating rate are shown in the ESI Fig. S9. Stage 2 and 3 are similar, showing increasing activation energies. These energies are typical for a crystal structure with guests in channels. The same tendency was observed in **H•IND** which is isostructural with **H•NAP**. (*ESI Fig. S10 and S11).*

Table 2 Thermal analysis results and activation energy ranges for the three stages of decomposition of **H•NAP**

Reaction Stage	Mass loss % Exp (calc.)	Activation energy range (kJ mol^{-1})
Stage 1	30.1 (29.5)	54.5 – 56.7
Stage 2	24.7 (24.8)	66.1 – 67.8
Stage 3	24.7 (24.8)	95.3 – 105.1

Experimental section

Preparation of Werner clathrate

The host compound, **H**, bis(isothiocyanato)tetrakis(4-vinylpyridine)nickel(II), was prepared by adding stoichiometric quantities of ethanolic solution of 4-vinylpyridine (20 ml, 0.01 M) to an ethanolic solution of nickel isothiocyanate (5 ml, 0.01 M). Blue crystals of $Ni(NCS)_2(C_7H_7N)_4$ were formed immediately and were filtered and allowed to air dry overnight.

Enclathration of any of the given guests via solution crystallisation was carried out by dissolving the host and the guest separately in warm alcohol, followed by addition of the guest solution to the host dropwise and stirring at a temperature of 50ºC for 30 minutes. The solution was cooled,

filtered and allowed to crystallise by slow solvent evaporation. Deep blue or violet crystals of each inclusion compound were formed.

Single crystal X-ray analysis

Intensity data of a selected single crystal for compounds **H•IND**, **H•NAP**, **H•AZU, H•FLU(I)**, **H•FLU(II)**, **H•ANT**, **H•PHE**, **H•PHE•BEN** and **H•PYR•MeOH** were collected on a Bruker DUO APEX II diffractometer[33] with graphite monochromated Mo $K_{\alpha 1}$ radiation (λ = 0.71073 Å) at 173 K using an Oxford Cryostream 700. Data reduction and cell refinement were performed using *SAINT-Plus.*[34] The space group was determined from systematic absences by *XPREP.*[35] The structure was solved using *SHELXS-97*[36] and refined using full matrix least squares methods in *SHELXL-97*[36] with the aid of the program *X-Seed.*[37] The hydrogen atoms bound to carbon atoms were placed at idealized positions and refined as riding atoms. In **H•FLU(II)** and **H•ANT** the guests were treated isotropically and the hydrogens were not added due to the high level of disorder. Diagrams and publication material were generated using *PLATON*,[38] *X-Seed* and *Mercury (3.1)*.[39] Crystal data and structure refinement parameters are given in Table 1. Supplementary crystallographic data for structures are in: CDC1431480 (H•IND); CCDC1431481 (H•NAP); CCDC1431482 (H•AZU); CCDC143143 (H•FLU(I)); CCDC1431484 (H•FLU(II)); CCDC1431485 (H•PHE•BEN); CCDC1431486 (H•PHE), CCDC1431487 (H•ANT) and CCDC1431488 (H•PYR•MeOH).

Solid-solid grinding experiments

Stoichiometric amounts of the host and guest were placed in a mortar and were ground at room or higher temperature as required for different time periods. The grinding was interrupted for a fixed amount of diamond powder to be added as internal standard before the product was analysed by a Bruker D8 X-ray powder diffractometer. The traces were compared with those of the starting materials and those generated from the single crystal structure. The rate constant and half-life of the reaction were determined from the graphic representation of the findings. The crystallinity of **NAP** did not change between 0 and 15 minutes grinding.

Co-crystallisation by slurry methodology

The slurry experiments were run at room temperature for 48 to 96 hours in water. The product was filtered, dried and analysed by PXRD. From the X-ray patterns, the reaction between the host and guest was determined by comparison with the pattern of the inclusion compound.

Melt experimentation

A mixture of stoichiometric amounts of the host and the guest were placed on the hot-stage microscope and the temperature was slowly raised 10 degrees above the guest's melting point and kept there for ten minutes and the product was analysed by powder X-ray diffraction.

Conclusions

The Werner clathrate $Ni(NCS)_2(4\text{-vinylpyridine})_4$ has been synthesised and used as a host in the synthesis of 9 inclusion compounds with a selection of seven polycyclic aromatic hydrocarbons (PAHs). Green chemistry methods were used to enclathrate these environmental contaminants with the Werner host.

Single crystal structural analysis revealed two types of crystal arrangements. Indene, naphthalene and azulene yield isomorphous structures ($Pna2_1$) with the guests in crossed channels down [100] and [010]. The azulene guest was disordered in the same way as described by Robertson and co-workers.[40] The remaining inclusion compounds all crystallised in $P\bar{1}$ space group with the guests located in channels along [010]. Disorder was observed in certain thiocyanato and vinyl groups as well as in anthracene, phenanthrene and fluorene guests.

The enhancement of green chemistry was pursued in the formation methods of corresponding compounds with grinding, slurrying or melt procedures. Intriguing results were obtained in the grinding experiments which proved to be successful. The success of compound formation by grinding was dependent on diffusion as shown by the guests naphthalene and azulene. The rate constant and half-life were determined for the reaction between the host with these two guests.

Product formation with slurry methods with naphthalene, indene and azulene were successful at 25ºC while with phenanthrene, fluorene and pyrene partial success was reached at 50ºC. These guests all possessed minimal solubility in water at the corresponding temperatures to which the success of these experiments were related.

Non-isothermal thermogravimetric analysis was used to determine the kinetics of thermal decomposition for the clathrate crystals of indene and naphthalene. The intercalate form of the compound was displayed by lower activation energy for the release of the guest than that of the loss of the host ligands.

Previously it was shown that the enclathration properties of Werner compounds may be altered by different crystallisation procedures but interestingly, this selected Werner host gives equivalent products when the ways of crystal formations are changed.

Acknowledgements

This work is based on the research supported in part by the National Research Foundation of South Africa for the grant, Unique Grant No. 93953 and No. 92763 and the authors wish to thank the NRF and the Cape Peninsula University of Technology for financial support. Any opinion, finding and

conclusion or recommendation expressed in this material is that of the author(s) and the NRF does not accept any liability in this regard. The authors declare that they have no conflict of interest.

Notes and references

[1] K. Tanaka and F. Toda, *Chem. Rev.*, 2000, **100**, 1025
[2] G. Nagendrappa, *Resonance*, 2002, **7**, 59
[3] T. Friščič, *Chem. Soc. Rev*., 2012, **41**, 3493
[4] T. Friščič and W. Jones, *Cryst. Growth. Des.*, 2009, **9**, 1621
[5] G.R. Desiraju, J.J. Vittal and A. Ramanan, *Crystal Engineering*, 2011, 79
[6] M. Lusi and L.J. Barbour, *Angew. Chem. Int. Ed.*, 2012, **51**, 1
[7] E. Batisai, M. Lusi, T. Jacobs and L.J. Barbour, *Chem. Commun.*, 2012, **48**, 12171
[8] J. Jacob, *Pure & Appl. Chem.*, 1996, **68**, 301
[9] A. Moissette, S. Marquis, I. Generb and C. Brémarda, *Phys. Chem. Chem. Phys.*, 2002, **4**, 5690
[10] M. Raters, and R. Matissek, *J. Agric. Food Chem.*, 2014, **62**, 10666
[11] J.-M. Lehn, *Supramolecular Chemistry Concepts and Perspectives*, Wiley-VCH: Weinham, Germany, 2009
[12] K.K. Arora and V.R. Pedireddi, *Tetrahedron*, 2004, **60**, 919-925
[13] E. Curtis, L.R. Nassimbeni, H.Su and J.H. Taljaard, *Cryst.Growth.Des*., 2006, **6**, 2716-2719
[14] A.D. Herrera-España, G. Campillo-Alvarado, P. Román-Bravo, D. Herrera-Ruiz, H. Höpfl and H. Morales-Rojas, *Cryst.Growth.Des*, 2015, **15**, 1572
[15] F. H. Allen, Acta Cryst., B58, 380-388, 2002
[16] J. Lipkowski, L. Gluzinski, K. Suwinska and G. D. Andreetti, *J. Incl. Phen.*, 1984, **2**, 327
[17] M.M. Wicht, N.B. Báthori and L.R. Nassimbeni, *Dalton. Trans.*, 2015, **44**, 6863
[18] W.D. Schaeffer, W.S. Dorsey, A. Skinner and C.G. Christian, *J.Am.Chem.Soc.*, 1957, **79**, 5870
[19] J. Lipkowski, in *Inclusion* Compounds, Academic Press, New York, 1984, vol.1, ch.3
[20] J.Lipkowski, in *Comprehensive Supramolecular Chemistry*, ed. D.D. MacNicol, F. Toda and R. Bishop, Elsevier Science, Oxford, 1996, vol.6, ch.20
[21] J. Lipkowski, K. Suwinska, J. Halt, A. Zielenkiewicz and W. Zielenkiewicz, *J. Inclusion Phenom.*, *Mol. Rec. Chem.*, 1984, **2**, 317
[22] M.H. Moore, L.R. Nassimbeni, M.L. Niven and M.W. Taylor, *Inorg. Chim. Acta*, 1986, **115**, 211
[23] M.H. Moore, L.R. Nassimbeni and M.L. Niven, *Inorg. Chem. Acta*, 1987, **131**, 45
[24] L.R. Nassimbeni, M.L. Niven and A.P. Suckling, *Inorg. Chim. Acta*, 1989, **159**, 209
[25] L. Lavelle and L.R. Nassimbeni, *J. Incl. Phenom. Mol. Rec. Chem.*, 1993, **16**, 25
[26] S. M. Soliman, Z. B. Elzawy, M. A. M. Abu-Youssef, J. Albering, K. Gatterer, L. Öhrström and S. F. A. Kettle, *Acta Cryst*., 2014, **B70**, 115.
[27] R.P. Rastogi, P.S. Bassi, S.L. Chadha, *J.Phys. Chem.*, 1963, **67**, 2569
[28] R.P. Rastogi and N.B. Singh, *J.Phys. Chem.*, 1968, **72**, 4446
[29] D. Braga, S.L. Giaffreda, F. Grepioni, A. Pettersen, L. Maini, M. Curzi and M. Polito, *Dalton Trans.*, 2006, 1249
[30] CRC Handbook of Chemistry and Physics, 87th Edition, 2006 – 2007, CRC Press
[31] Lange's Handbook of Chemistry, 12th Edition, 1979, McGraw-Hill Book Company
[32] J.H. Flynn and L.A. Wall, *Polymer Lett.*, 1966, **4**, 323
[33] Bruker 2005. APEX2. Version 1.0-27. Bruker AXS Inc., Madison, Wisconsin, USA.
[34] Bruker 2004. SAINT-Plus (including XPREP). Version 7.12. Bruker AXS Inc., Madison, Wisconsin, USA.
[35] Bruker 2003, XPREP2. Version 6.14. Bruker AXS Inc., Madison, Wisconsin, USA.
[36] G. M. Sheldrick, SHELXS-97 and SHELXL-97 *Programs for crystal structure determination and refinement*. University of Göttingen, 1997.
[37] L. J. Barbour, *J. Supramol. Chem*., 2001, 1, 189.
[38] A. L. Spek, *PLATON, A Multipurpose Crystallographic Tool*, Utrecht University, Utrecht, The Netherlands, 2008.
[39] C. F. Macrae, I. J. Bruno, J. A. Chisholm, P. R. Edgington, P. McCabe, E. Pidcock, L. Rodriguez-Monge, R. Taylor, J. van de Streek, P. A. Wood, J. *Appl. Cryst.*, 2008, 41, 466
[40] J. M. Robertson, H. M. M. Shearer, G. A. Sim and D. G. Watson, *Acta Cryst.*, 1962, **15**, 1

Graphical Abstract

Werner clathrate formation with polyaromatic hydrocarbons: comparison of different crystallisation methods

Merrill M. Wicht, Hong Su, Nikoletta B. Báthori* and Luigi R. Nassimbeni

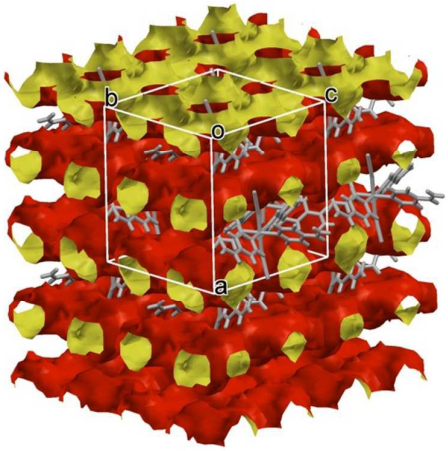

Werner clathrates of bis-isothiocyanato tetrakis-vinylpyridine nickel (II), with seven polyaromatic hydrocarbons were formed by a variety of crystallisation methods such as solution crystallisation, grinding, slurrying and co-melting; single crystal structures and kinetic properties are discussed.